FUNGAL BIOLOGY 116 (2012) 1052–1063

British Mycological Society promoting fungal science

journal homepage: www.elsevier.com/locate/funbio

Differences in crystalline cellulose modification due to degradation by brown and white rot fungi

Anne Christine Steenkjær HASTRUP[a,*], *Caitlin HOWELL*[b], *Flemming Hofmann LARSEN*[c], *Noppadon SATHITSUKSANOH*[d], *Barry GOODELL*[e], *Jody JELLISON*[f]

[a]*Department of Biotechnology, Chemistry and Environmental Engineering, Aalborg University, A.C. Meyers Vænge 15, 2450 Copenhagen SV, Denmark*
[b]*Institute of Applied Physical Chemistry, University of Heidelberg, INF 253, 69120 Heidelberg, Germany*
[c]*Department of Food Science, University of Copenhagen, Rolighedsvej 30, 1958 Frederiksberg C, Denmark*
[d]*Joint BioEnergy Institute, Lawrence Berkeley National Laboratory, Emeryville, CA 94608, USA*
[e]*Department of Sustainable Biomaterials, 230 Cheatham Hall, Virginia Tech, Blacksburg, VA 24061, USA*
[f]*Virginia Agricultural Experiment Station, College of Life Sciences and Agriculture, 104 Hutcheson Hall, Virginia Tech, Blacksburg, VA 24061, USA*

ARTICLE INFO

Article history:
Received 15 May 2012
Received in revised form
11 July 2012
Accepted 27 July 2012
Available online 8 August 2012
Corresponding Editor:
Daniel C. Eastwood

Keywords:
^{13}C CP/MAS NMR
Cellulose crystallinity
d-spacing
Wood decay
X-ray diffraction

ABSTRACT

Wood-decaying basidiomycetes are some of the most effective bioconverters of lignocellulose in nature, however the way they alter wood crystalline cellulose on a molecular level is still not well understood. To address this, we examined and compared changes in wood undergoing decay by two species of brown rot fungi, *Gloeophyllum trabeum* and *Meruliporia incrassata*, and two species of white rot fungi, *Irpex lacteus* and *Pycnoporus sanguineus*, using X-ray diffraction (XRD) and ^{13}C solid-state nuclear magnetic resonance (NMR) spectroscopy. The overall percent crystallinity in wood undergoing decay by *M. incrassata*, *G. trabeum*, and *I. lacteus* appeared to decrease according to the stage of decay, while in wood decayed by *P. sanguineus* the crystallinity was found to increase during some stages of degradation. This result is suggested to be potentially due to the different decay strategies employed by these fungi. The average spacing between the 200 cellulose crystal planes was significantly decreased in wood degraded by brown rot, whereas changes observed in wood degraded by the two white rot fungi examined varied according to the selectivity for lignin. The conclusions were supported by a quantitative analysis of the structural components in the wood before and during decay confirming the distinct differences observed for brown and white rot fungi. The results from this study were consistent with differences in degradation methods previously reported among fungal species, specifically more non-enzymatic degradation in brown rot *versus* more enzymatic degradation in white rot.

Introduction

There is a growing demand for ecologically sustainable fuels and biochemicals. The conversion of woody biomass to fill this need is promising. The difficulty of efficiently hydrolyzing the recalcitrant crystalline cellulose in this material has proven to be a major barrier (Himmel *et al.* 2007). Wood decay fungi are among the most effective bioconverters of native

* *Corresponding author*. Tel.: +1 45 2023 5937; fax: +45 9940 2594.
E-mail addresses: acsh@bio.aau.dk (A. C. S. Hastrup), chowell@seas.harvard.edu (C. Howell), fhl@life.ku.dk (F. H. Larsen), nsathitsuksanoh@lbl.gov (N. Sathitsuksanoh), Goodell@vt.edu (B. Goodell), jody@vt.edu (J. Jellison)
URL: http://www.sustainablebiotechnology.aau.dk
1878-6146/$ – see front matter
http://dx.doi.org/10.1016/j.funbio.2012.07.009

cellulose, playing an important role in the nutrient cycling of forest ecosystems, as well as being the major cause of decay of in-service wood (Baldrian & Valkov 2008). This has led to a long-lasting interest in a more thorough understanding of the mechanisms employed by these fungi.

Basidiomycete wood decay fungi are traditionally grouped into two categories: brown rot and white rot. Although originally classified based upon the colour of the wood following decay, these two groups are now known to have significantly different approaches to degradation. Brown rot fungi preferentially degrade cellulose and hemicelluloses, and at least some species extensively modify the lignin (Yelle *et al.* 2008, 2011; Arantes *et al.* 2011). The degradation mechanism is initiated by non-enzymatic processes based upon the generation of hydroxyl radicals from the reaction between hydrogen peroxide and ferrous iron, the Fenton reaction:

$$H_2O_2 + Fe^{2+} \rightarrow {}^{\bullet}OH + OH^{-} + Fe^{3+}$$

The radicals quickly depolymerize nearby wood components, resulting in a rapid strength loss with little measurable weight loss in the wood early in the decay process (Goodell *et al.* 1997; Hyde & Wood 1997). Enzymatic action then follows. Brown rot fungi initially decompose pectin and hemicelluloses followed by cellulose degradation. Lignin is modified in the process (Goodell *et al.* 2002; Arantes *et al.* 2011).

The mechanisms of 'simultaneous' white rot fungi seemingly rely more heavily on enzymatic degradation of hemicelluloses, cellulose, and lignin, with more limited diffusion of non-enzymatic degradation systems, leading to a more thorough degradation of wood (Zabel & Morrell 1992; Arantes *et al.* 2011) reflected in simultaneous weight loss and depolymerization of cellulose (Kleman-Leyer *et al.* 1992). White rot fungi remove the three major wood components either simultaneously or selectively by preferentially attacking the lignin and hemicelluloses followed by hydrolysis of cellulose.

Cellulose chains in wood are arranged in microfibrils with regions containing crystalline structure as well as areas of less ordered cellulose. The latter region is often referred to as amorphous or non-crystalline (Larsson *et al.* 1997; Thygesen *et al.* 2005). However, elucidation of the organization of these regions with respect to one another has proven to be quite complex (Larsson *et al.* 1997; Thygesen *et al.* 2011). One model suggests an arrangement with crystalline cellulose in the interior of the microfibrils and the less ordered cellulose chains towards the surface (Newman & Hemmingson 1995; Nishiyama 2009). However, the actual distribution of the various crystalline cellulose structures remains to be clarified.

Work examining changes in wood crystallinity during brown rot decay shows an initial increase in apparent percent crystallinity as amorphous wood components, i.e. hemicelluloses and non-crystalline cellulose, are removed. This is then followed by a decline in percent crystallinity as the crystalline cellulose material begins to break apart (Howell *et al.* 2007, 2009a). Decrease in the average distance between the crystalline planes (*d*-spacing) during decay is attributed to the removal of more loosely packed outer cellulose chains as well as a possible rearrangement of the remaining crystalline material into a more energetically favourable, tightly packed state (Howell *et al.* 2007, 2009a, 2011). Changes in cellulose crystallinity including structural spacing of the crystalline planes caused by white rot fungi during decay have, to the best of our knowledge, not yet been reported.

The aim of this study was to compare the effects of brown and white rot decay on crystalline cellulose. This was accomplished by examining wood decayed over time using ^{13}C solid-state cross-polarization (CP), magic-angle-spinning (MAS) nuclear magnetic resonance (NMR) spectroscopy and X-ray diffraction (XRD), while the wood composition was analyzed by acid hydrolysis using high performance liquid chromatography (HPLC). These techniques give complimentary information about the changes occurring in wood in terms of cellulose crystallinity and crystal lattice spacing, as well as structural changes and alterations in the chemical composition. The fact that the former two methods are non-destructive and can be applied directly on dried wood powder without further modification is an advantage, as it eliminates the need for chemical treatment of the wood substrate, which may alter the state of the crystalline cellulose or other wood polymers.

Materials and methods

Growth conditions and wood processing

The organisms used in this study were chosen to represent two types of brown rot decay and two types of white rot decay. The brown rot species used were *Gloeophyllum trabeum* (ATCC 11539), a low oxalic acid (OA) accumulator and high phenolate (iron-chelator) accumulator and *Meruliporia incrassata* (MFS-1), a high OA accumulator and low phenolate accumulator (Green & Clausen 2003; Hastrup 2011; Hastrup et al. 2012a, b). The white rot species used were *Irpex lacteus* (ATCC 60993), a simultaneous lignin degrader, and *Pycnoporus sanguineus* (ATCC 24598), a selective lignin degrader.

As the substrate, Red Maple strands from both heart- and sapwood were combined into bundles of approximately $20 \times 30 \times 10$ mm^3 by stacking the strands and securing them with nylon cord (Howell *et al.* 2009b). Fungi were grown at approximately 90 % relative humidity at room temperature in modified American Society for Testing and Materials (ASTM) soil-block jars (AWPA 2003; Howell *et al.* 2007): four 1 cm^2 squares of inoculum were taken from the outer edge of 2-week-old fungal cultures and placed at the corners of birch feeder strips on top of one cup of a 1:1:1 mixture of potting soil, sphagnum peat moss, and horticultural grade vermiculite, wetted with deionized water. Each wood sample was weighed prior to incubation and one was placed in each jar after the mycelial mat had covered the feeder strips. Fungi were allowed to grow for 3, 6, 9 or 12 weeks after the addition of the wood block. There were three replicates per fungus per harvest, as well as uninoculated controls.

After harvesting, the wood was brushed free of mycelium, dried for 48 h at 95 °C and weighed. The wood substrate was then ground in a Wiley Mill to pass through a standard 40-mesh screen (420 μm). For XRD measurements, this powder was then pressed into a cylindrical wafer 25 mm in

diameter and 4.3 mm thick. For NMR analysis the powder was used unaltered.

Carbohydrate and lignin assays

The structural carbohydrate composition of all samples was determined with modified quantitative saccharification (QS) procedure (Moxley & Zhang 2007) employing H_2SO_4 in a two-step acid hydrolysis. Monomeric sugars were measured by a Shimadzu HPLC with a Bio-Rad Aminex HPX-87P column (Richmond, CA, USA) equipped with refractive index (RI) detector. The column was operated with deionized water as the mobile phase at 80 °C and a flow rate of 0.6 mL min^{-1}. Klason lignin and ash were measured according to the standard National Renewable Energy Laboratory (NREL) biomass protocol (Sluiter *et al.* 2008). The results were adjusted according to the recorded density loss.

XRD spectral analysis

Wood wafers were examined using a Panalytical X'Pert XRD machine (Panalytical, Netherlands) with symmetric θ–2θ Bragg–Brentano scattering geometry according to Howell *et al.* (2007, 2009a). Nickel filtered *Kα* radiation with a wavelength of 1.542 ≈ was used to perform θ–2θ scans. The incident beam was passed through a fixed divergence slit of 1/16° and an anti-scatter slit of 1/8°, as well as a 15-mm mask. The diffracted beam was passed through a size 5.0 anti-scatter slit. Data were collected in the 2θ-range 5–35° with a step size of 0.01°. The scans proceeded at 0.08° s^{-1} (150 s $step^{-1}$). Percent crystallinity of the wood material was calculated from the XRD data by comparing the area of the crystalline regions to the total area. Two different methods were used: a standard least-squares peak fitting method with an amorphous standard (Thygesen *et al.* 2005), and a Rietveld analysis (Rietveld 1969) using the cellulose I_β crystal structure published by Nishiyama *et al.* (2002). The results from the two methods did not show significant differences and values from the Rietveld analyses are presented.

The average distance between the crystal planes was calculated using Bragg's law:

$$2d\sin\theta = n\lambda \quad (1)$$

where d represents the distance between the crystal planes, θ the angle between the planes and the incoming X-rays, λ the wavelength of the X-rays, and n an integer. The value obtained for the d-spacing between the 200-crystal planes was then doubled to take into account the body-centred crystal arrangement providing a value reflecting the distance between β-D-glucan molecules in a single unit cell.

Solid-state ^{13}C CP/MAS NMR spectroscopy and principal component analysis (PCA)

NMR spectra were obtained and analyzed from wood powder after 9 and 12 weeks of fungal decay, as well as non-decayed controls. Due to accelerated decay in wood inoculated by *Meruliporia incrassata*, only samples from 9 weeks were analyzed, as at this point the weight loss in these samples was similar to the three other species after 12 weeks of decay. Seventy milligram (approximately) of wood powder as used for acquisition of the solid-state NMR spectra.

The ^{13}C CP MAS NMR spectra were recorded on a Bruker Avance 400 (9.4 T) spectrometer (Bruker BioSpin Gmbh, Rheinstetten, Germany), operating at Larmor frequencies of 400.13 and 100.62 MHz for ^{1}H and ^{13}C, respectively. The experiments were carried out using a double-tuned (CP/MAS) probe equipped with a 4 mm (o.d.) rotor. ^{1}H and ^{13}C rf-field strengths of 80 kHz were utilized during both two-pulse phase modulation (TPPM)-^{1}H-decoupling (Bennett *et al.* 1995), and CP. The variable amplitude CP scheme (Peersen *et al.* 1993) was employed to enhance the CP performance during fast spinning. All spectra were acquired at room temperature using a spin-rate of 8 kHz, a contact time of 1.0 ms, an acquisition time of 37.3 ms, a recycle delay of 3 s and 1000 scans. Prior to Fourier transformation the free induction decays (FID) were apodized by Lorentzian line broadening of 10 Hz. All spectra were referenced (externally) to the carbonyl resonance in α-glycine at 176.5 parts per million (ppm).

Data analysis

The ^{13}C CP/MAS spectra were examined by PCA (Wold *et al.* 1987) using the built-in PCA procedure in PLS toolbox 5.5 in Matlab 7.9.0.529. Prior to PCA the data from the 24 NMR spectra were mean centred. By mean centring the average spectrum is subtracted from each experimental spectrum prior to PCA. Therefore (0,0) in the PCA score plot will represent the position of the (artificial) average spectrum. No other normalization procedures were applied as all spectra were recorded under identical experimental conditions.

The ratio of interior to surface chains was calculated as:

$$R = \frac{[86 - 92\ \text{ppm}]}{[80 - 86\ \text{ppm}]} \quad (2)$$

The statistical analyses were performed using Student's two-tailed *t*-test or conducted by a three- or four-way analysis of variance (ANOVA) analysis of variance (general linear model) (SAS version 9.2, SAS Institute Inc., Cary, NC, USA). *P*-values ≤0.05 were considered significant. Results are presented as the mean value of the replicates ± standard error in tables. In graphics standard error is represented as vertical bars ($n = 3$).

Results and discussion

XRD detects the interference pattern created when x-rays encounter the regularly spaced crystalline cellulose planes in wood and has been used for decades as a rapid, non-destructive method for observing the crystalline portion of wood. It is one of the primary tools used in the determination of the conformation and structure of cellulose microfibrils (Cullity 1978; Cave 1997; Lichtenegger *et al.* 1999). XRD can be used to follow the changes occurring in cellulose in terms of crystallinity and crystal lattice spacing (*d*-spacing) (Cave 1997; Lichtenegger *et al.* 1999; Howell *et al.* 2007, 2009a). Solid-state ^{13}C CP/MAS NMR spectroscopy combined with proton decoupling can be used to observe various components within wood such as ordered and disordered cellulose, different crystal forms of cellulose, as well as detect hemicelluloses and lignin molecules (VanderHart & Atalla 1984; Newman &

Hemmingson 1995; Bardet *et al.* 2009; Martinez *et al.* 2009). NMR is useful in describing distinct structural changes in wood components during the decay process (Howell *et al.* 2011).

Where XRD is capable of giving a picture of the overall changes occurring in the overall amount and lattice spacing of the crystalline cellulose (Howell *et al.* 2007), NMR is able to depict more clearly the changes in the surrounding wood polymers as well as whether the changes in the crystalline cellulose are occurring in the interior or on the exterior of the crystalline fibrils (Newman & Hemmingson 1995). Therefore the combination of ^{13}C CP/MAS NMR and XRD for structural analysis of cellulose and surrounding wood polymers is a powerful tool. By comparing the progression of decay caused by brown and white rot fungi with both techniques it is possible to gather a more complete picture of what is occurring on the molecular scale in the cellulose and surrounding polymers, as XRD and NMR function by probing complimentary aspects of the molecular structure of the wood substrate.

One of the major drawbacks to both methods is that other wood components such as hemicelluloses and lignin can interfere with signal from the cellulose, or *vice-versa*, making the results difficult to interpret. In XRD spectra, the amorphous portion of the wood has to be estimated and subtracted from the crystalline portion to obtain a realistic picture of the cellulose alone. In NMR spectra, lignin, and hemicelluloses have residues in the regions assigned to cellulose structures. Nevertheless, with the information gained by combining the information from both methods it is possible to cross-reference the data to a certain extent to overcome these limitations, ultimately allowing for a thorough analysis of the changes occurring in wood structure and crystallinity following fungal decay.

Degradation efficiency

Weight loss measurements were performed as a measure for the removal of the wood components although these measurements did not take into account the structural changes occurring in the wood or give information on which components were affected. The two groups of basidiomycetes, brown and white rot, preferentially grow on softwood and hardwood tree species, respectively (Zabel & Morrell 1992; Tuor *et al.* 1995). However, a single type of wood was preferential in this study for both types of fungi to allow direct comparisons utilizing a uniform substrate. White rot fungi are less aggressive in softwood compared to brown rot fungi (Pandey & Pitman 2003) whereas in hardwood the decay is comparable to brown rot fungi (Howell *et al.* 2009a, b). For this reason hardwood was chosen as substrate. Weight losses for the brown rot *Gloeophyllum trabeum* and the two white rot fungi were found to be similar throughout the decay period (Table 1). At 12 weeks *G. trabeum* caused lower weight loss in the hardwood blocks compared to analysis of the growth of this strain on coniferous wood (Hastrup 2011). The second brown rot species, *Meruliporia incrassata*, showed enhanced weight loss at the early stages of decay compared to the other three species, but at 12 weeks there was no statistically significant difference in the degree of decay caused by the four fungi tested, with all showing an average weight loss in the wood samples of approximately 30 % ($P > 0.05$) (Table 1).

Table 1 – Wood block weight losses (%) following fungal decay.

	Week 3	Week 6	Week 9	Week 12
G. trabeum	6.8 (0.4)[a]	14.2 (2.4)	21.5 (2.7)	28.0 (0.9)
M. incrassata[b]	12.9 (2.6)	33.9 (3.4)	37.7 (2.6)	37.6 (4.1)
I. lacteus	2.8 (0.6)	10.0 (0.8)	21.4 (0.7)	30.1 (0.9)
P. sanguineus	2.9 (0.2)	9.4 (0.7)	16.7 (0.6)	31.8 (4.6)
Control	−0.03 (0.01)	−0.1 (0.01)	−0.1 (0.01)	0.01 (0.07)

a Standard error is given in parenthesis.
b Data on percent weight loss, percent crystallinity, and changes in *d*-spacing from *M. incrassata* decayed samples has been presented in Howell *et al.* 2011 in a different context.

Changes in wood composition

Brown rot fungi caused a greater level of degradation of the hemicellulose components as represented by xylan and mannan compared to the white rot fungi (Fig 1). Also, the concentration of cellulose (glucan) was proportionally reduced in wood degraded by brown rot fungi despite overall similar mass reduction, which can be explained by elevated lignin removal in white rot fungi (Zabel & Morrell 1992). The variation in cellulose concentration at earlier time points, measured between *Meruliporia incrassata* and *Gloeophyllum trabeum* is attributed to the difference in weight loss. The same elevated removal of hemicelluloses by *M. incrassata* was observed at early stages of decay but was less apparent at weight losses above 20 % as most accessible hemicelluloses are degraded at this point (Curling *et al.* 2001; Howell *et al.* 2009a). Preferential degradation of lignin by *Pycnoporus sanguineus* was observed early in the decay process as this organism removed significantly more lignin than *Irpex lacteus* after 6 weeks of decay ($P = 0.04$). The four carbohydrate components shown represent only some of the elements in the wood and therefore do not total to 100 %.

The ^{13}C CP/MAS NMR spectrum of the red maple control sample is shown in Fig 2, and resonance assignments are presented in Table 2. Resonance 12 at 21.5 ppm is assigned to the methyl carbon of the acetyl group in hemicelluloses. The region between 60 and 106 ppm is dominated by intense resonances, labelled 4–10, primarily originating from cellulose, but resonances from hemicelluloses are also observable in this region. The resonances at ~89 ppm (labelled 5) and ~65 ppm (labelled 9) originate from C4 and C6, respectively, in ordered interior cellulose, while the resonances at ~84 ppm (labelled 6) and ~63 ppm (labelled 10) are due to C4 and C6, respectively, in more disordered, surface cellulose (Atalla & VanderHart 1999). It should be noted that resonances from lignin are also present in the spectral region 75–92 ppm and are partially overlapping with resonances from cellulose and hemicelluloses. Resonance 4 at ~105.2 ppm is primarily originating from C1 in cellulose, although some overlapping with anomeric carbons of hemicelluloses cannot be excluded. Lignin-specific resonances are observed at 56.5 ppm (methoxy groups) and in the region of 120–160 ppm (aromatic carbons in lignin). The resonance at ~172.8 ppm (labelled 1) originates from carbonyl carbons in acid or ester groups of the hemicelluloses.

Structural alterations caused by the wood decay fungi are illustrated by representative ^{13}C CP/MAS NMR spectra recorded

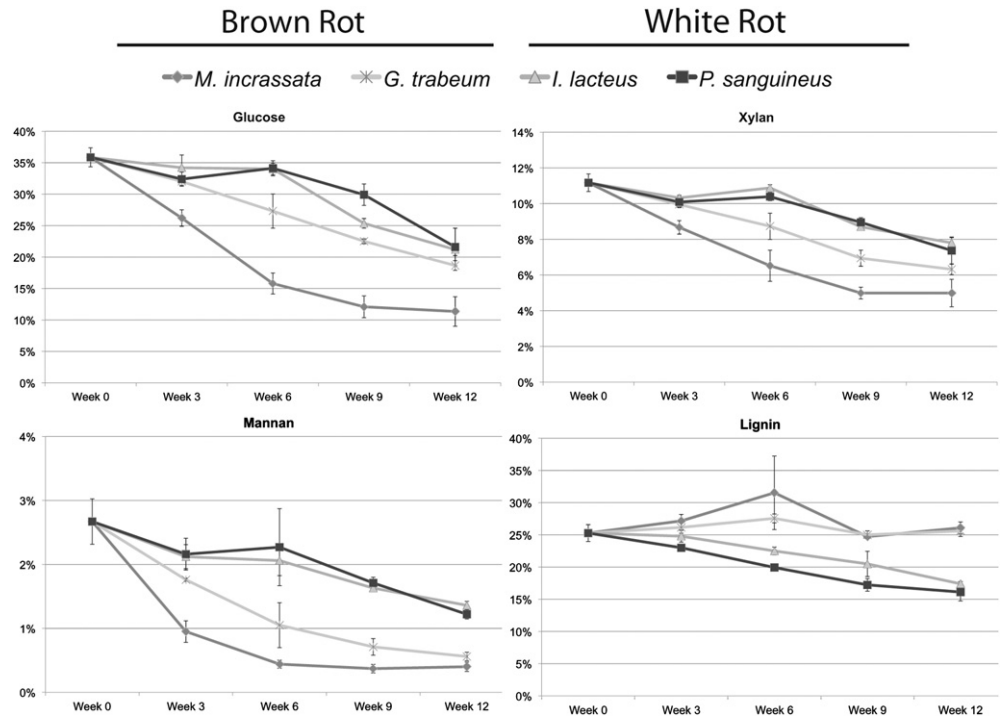

Fig 1 – Wood component analysis. Relative percentage carbohydrate and lignin composition of wood degraded by the two brown rot fungi, *M. incrassata* (circle) and *G. trabeum* (star) and the two white rot fungi, *I. lacteus* (triangle) and *P. sanguineus* (square) for 3, 6, 9 or 12 weeks. Week 0 data represent uninoculated control wood samples. Bars represent standard error.

under identical conditions (Fig 2). From direct comparison the effect of fungal degradation on various component specific resonances can be followed. It is observed that the effect of brown rot fungi is the selective removal of the carbohydrates and the effect of the white rot fungi is the degradation of lignin.

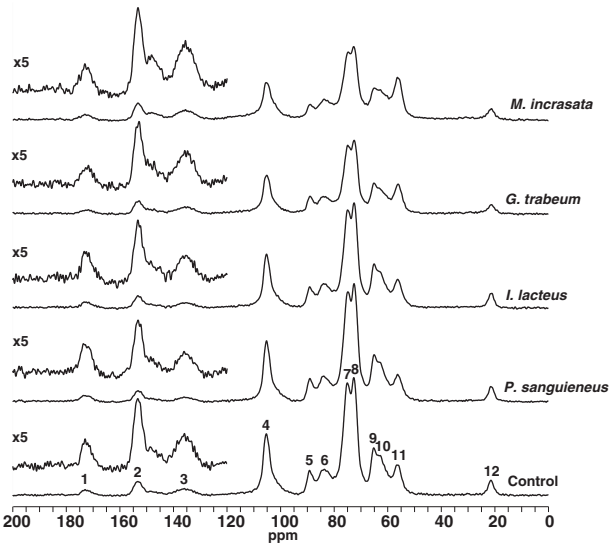

Fig 2 – Comparative NMR spectra. ^{13}C CP MAS spectra of red maple inoculated with the four wood decay fungi and a red maple control sample. Inserts of the spectral range 120–200 ppm have been vertically scaled by a factor of five. The numbers refer to the assignment given in Table 2.

In order to obtain a further overview of the differences among the samples, the NMR spectra were subjected to PCA. The result is presented in Fig 3. Fig 3A displays the PCA score plot of the ^{13}C CP/MAS spectra. It is observed that the samples tend to cluster according to fungal species. The main variation in the spectra (91.17 %) is described by principal component 1 (PC1) whereas a smaller part (5.86 %) is described by PC2. Together the two PCs describe 97 % of the spectral variation. The underlying spectral features (loadings) describing the PCs are shown in Fig 3B. From this it is observed that PC1 corresponds to a spectrum that can be described primarily as a difference

Table 2 – Resonance assignment of the ^{13}C CP/MAS spectrum adapted from Bardet *et al.* 2009.

Resonance number	Chemical shift (ppm)	Assignments
1	172.8	Carbohydrate; –COO–R, CH_3–COO–
2	153.1	Lignin
3	135.8	Lignins
4	105.3	Carbohydrates; C1
5	89.2	Carbohydrates; C4
6	84.2	Lignins; Carbohydrates; C4
7	75.1	Lignins; Carbohydrates; C2, 3, 5
8	72.7	Carbohydrates; C2, 3, 5
9	65.2	Carbohydrates; C6
10	63.3	Lignins; Carbohydrates; C6
11	56.5	Lignins; OCH3
12	21.5	Carbohydrates; CH3–COO–

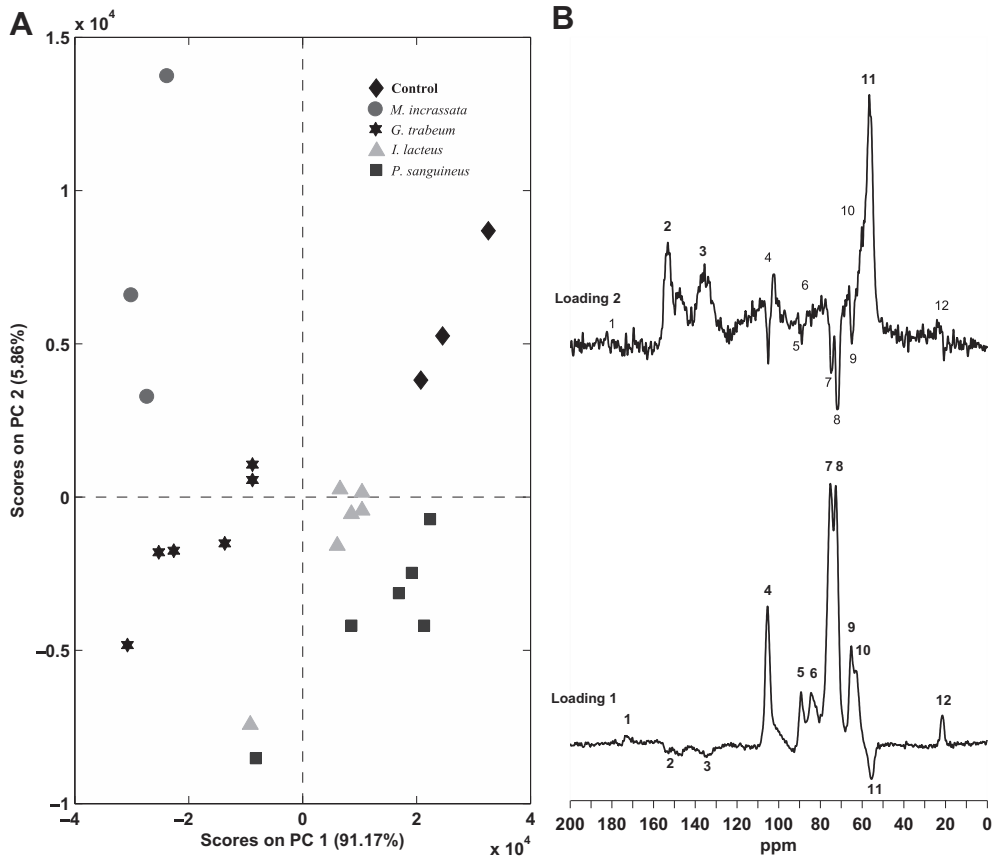

Fig 3 – Combined changes in polysaccharides and lignin. PCA of the ^{13}C CP/MAS spectra of the spectral range 0–200 ppm using samples from week 9 (all fungi) and week 12 (only *G. trabeum*, *I. lacteus*, *P. sanguineus*, controls). Part (A) displays the score plot, and part (B) the corresponding loadings for the selected PCs. In part (B) assignments (Table 2) are included.

between the sum of cellulose and hemicelluloses and a small amount of lignin. Therefore, a PC1 score smaller than that of the control samples is reflective of a reduced content of cellulose and hemicelluloses and a slightly increased amount of lignin. The loading for PC2 corresponds to a difference spectrum between lignin (Bardet *et al.* 2009) (positive intensity) and a small amount of crystalline cellulose (negative intensity).

Differences in degradation patterns between the brown and white rot fungi are illustrated in the score plot (Fig 3A). The brown rot fungi exhibit a significantly higher reduction in cellulose and hemicellulose content compared to the white rot fungi at similar weight losses (Table 1). This was also confirmed by the sugar analysis of samples at 12 weeks of fungal degradation (Fig 1). It has been suggested that the more thorough initial degradation of polysaccharides by brown rot fungi compared to white rot fungi is due to the combined effect of non-enzymatic and enzymatic processes (Goodell *et al.* 1997; Hyde & Wood 1997; Martinez *et al.* 2009; Hastrup *et al.* 2011). The tight structure of highly crystalline cellulose fibrils and the surrounding hemicellulose sheath leaves too little space for enzymes to initiate the hydrolysis process anywhere within the cellulose crystal (Flournoy *et al.* 1991; Arantes & Saddler 2010). However, the free radical stream generated from the non-enzymatic low molecular weight modified Fenton reaction is known to increase the porosity of wood, enabling subsequent access of the enzymes to the wood structures and facilitating the further depolymerization of the cellulose chains (Baldrian 2008; Arantes *et al.* 2011). White rot fungi rely on surface hydrolysis of the microfibrils (Zhao *et al.* 2007) and depolymerize holocellulose and lignin only to the extent that the product is used in their metabolism. The result is a steady decrease in degree of polymerization of the wood cellulose that could cause the observed slower change (Cowling 1961; Arantes & Saddler 2010) seen in Figs 1 and 3A.

In Fig 3A, PC2 mainly describes changes primarily related to lignin. Compared to the control samples, *M. incrassata* caused no measurable change in total/quantitative lignin signals whereas the resonances from the different lignin structures were lower in wood samples decayed by *G. trabeum*, *I. lacteus*, and *P. sanguineus*, with no notable difference between these three species. The fact that the white rot species showed a lower amount of lignin than observed in *M. incrassata* was also seen in the lignin analysis (Fig 1). However, the differences between *M. incrassata* and *G. trabeum* were not supported by the lignin measured in Fig 1 the reason being that the analysis for determining the amount of Klason lignin reveals the relative amount of lignin while NMR analysis is sensitive to specific structural changes in lignin undergoing degradation. This indicates physiological differences in the decay mechanism between the two brown rot fungi (Hastrup 2011; Hastrup *et al.* 2012a, b). It is generally agreed that brown rot fungi cause modification of lignin by demethylation and

demethoxylation *via* the hydroxyl radicals from Fenton chemistry aided by fungal chelators (Goodell *et al.* 1997; Hammel *et al.* 2002), whereas white rot fungi have the potential to produce a complete mineralization of lignin (Arantes *et al.* 2011; Martínez *et al.* 2011), however, species variation among brown rot fungi is still being defined (Hastrup *et al.* 2012a, b). The fact that equivalent results were observed in the NMR spectra between the two white rot fungi and *G. trabeum* does not prove that lignin modifications are performed by the identical mechanism. The white rot fungi cause an initial demethylation similar to *G. trabeum*, albeit most likely by different pathways (Martínez *et al.* 2005; Arantes *et al.* 2011) and it is known the lignin is depolymerized and then repolymerized in modification caused by some brown rot fungi (Yelle *et al.* 2008). This modification of lignin 'inter-unit linkages' by *G. trabeum* was also suggested by VanderHart & Atalla (1984).

Examining the changes in wood components by solid-state NMR and sugar analysis verified the standard brown and white rot decay patterns suggested for the brown and white rot fungi species included in this study. However, two important observations with direct implications for the modification of the crystalline cellulose were made: first, that both brown rot species aggressively attacked the polysaccharides despite different decay rates, as seen by the steady and nearly parallel decreases in xylan and mannan (Fig 1). Second, that the brown rot fungus *G. trabeum* reduced the lignin signal to a similar level as that observed for the white rot fungi (Fig 3) and was likely caused by demethoxylation and depolymerization of the lignin by this species. This was not observed in wood degraded by *M. incrassata*.

Changes in crystalline cellulose

The changes in percentage of the wood substrate consisting of crystalline cellulose (% crystallinity) were measured with XRD. The raw spectra were highly comparable to those published for wood (Thygesen *et al.* 2005; Howell *et al.* 2007), and the processed results are shown in Fig 4. *Meruliporia incrassata* caused the highest decrease in crystallinity, resulting in a decrease of ~10 % after 12 weeks of decay, followed by *Gloeophyllum trabeum* and *Irpex lacteus* with ~3.5 % and ~1.8 %, respectively (Fig 4). *Pycnoporus sanguineus* is the only strain which displayed a marked increase in crystallinity at week 6 and week 9.

Recent studies using the same strains of brown rot fungi grown on softwood showed a brief increase in wood percent crystallinity at ~20 % weight loss (Howell *et al.* 2007, 2009a). The cause was believed to be the removal of hemicelluloses and easily available non-crystalline cellulose early in the decay process, resulting in a greater apparent signal from the remaining crystalline material. The absence of this trend in the current data could be due to the use of hardwood, as these fungi are known to have a preference for softwood (Highley 1976; Tuor *et al.* 1995). The better adaptation to softwood may allow brown rot fungi to cause a quicker and more efficient degradation of non-crystalline softwood materials including the hemicelluloses compared to hardwood, resulting in the brief increase in crystallinity in that type of substrate. The fact that this did not occur on the hardwood is supported by the monosaccharide analysis (Fig 1) showing an almost simultaneous decrease in cellulose and hemicelluloses by the brown rot fungi.

The XRD data showed a significant difference at week 12 between the percent crystallinity of wood degraded by *M. incrassata* and wood degraded by *G. trabeum* (Fig 4). This is most likely due to the stage of decay. At this point the weight loss for *M. incrassata* was 37.6 % (±4.1 %), as compared to 28.0 % (±0.9 %) for *G. trabeum*. This is low for *G. trabeum* but, as noted above, this may be due to the hardwood substrate (Howell *et al.* 2011). However, non-enzymatic processes also are known to vary between these two fungal species. For example, *G. trabeum* generally accumulate lower amounts of OA than *M. incrassata* (Green & Clausen 2003; Hastrup *et al.* 2012a, b). Many roles have been proposed for OA in wood degradation, including direct acid hydrolysis, iron translocation, and precipitation of calcium from wood cell wall (Dutton & Evans 1996; Goodell *et al.* 1997, 2002; Hastrup *et al.* 2005, 2006, 2011; Schilling & Jellison 2006). The indirect effect of OA as a pH reducer is expected to enhance the non-enzymatic degradation mechanisms (Arantes & Saddler 2010; Hastrup *et al.* 2011). OA can also act by complexing ferric iron and facilitating translocation of iron into environments of more neutral pH. At the more neutral pH fungal (phenolate) with greater affinity can sequester and reduce the iron for use in Fenton chemistry (Goodell *et al.* 1997; Arantes *et al.* 2009). The relatively high level of accumulation of OA observed with *M. incrassata* may be contributing to the observed rapid decrystallization of cellulose and removal of hemicelluloses.

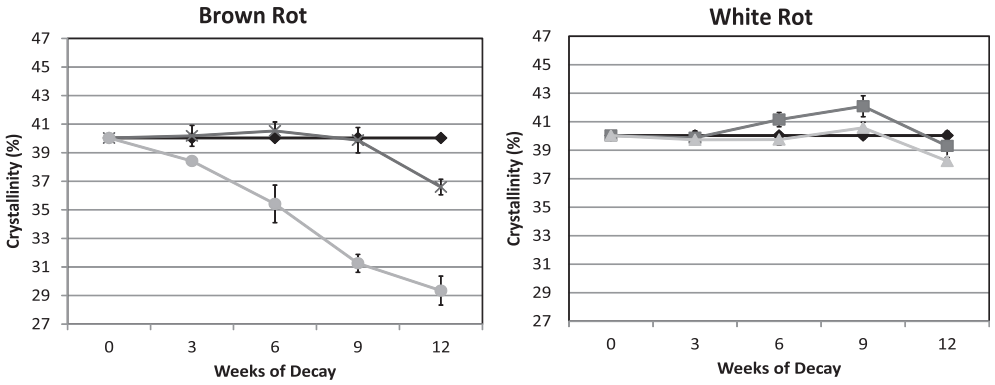

Fig 4 – Changes in crystallinity. Percent crystallinity determined by XRD data for wood decayed by the brown rot fungi *M. incrassata* (circle) and *G. trabeum* (star) (left), and the white rot fungi *I. lacteus* (triangle) and *P. sanguineus* (square) (right) *versus* undecayed controls (diamond). Data for *M. incrassata* has been previously published (Howell *et al.* 2011).

Pycnoporus sanguineus was found to cause a significant increase in crystallinity compared to *I. lacteus*. The relative increase in crystalline cellulose becomes clear at week 6 ($P = 0.087$), and is significant by week 9 ($P = 0.043$). This is likely due to the differences in type of white rot decay, i.e. selective *versus* simultaneous lignin degradation. The simultaneous degradation performed by *I. lacteus* results in the removal of hemicelluloses, lignin, and cellulose at approximately equal rates and might cause the steady decrease in the percent crystallinity observed. The limited change in percent crystallinity in wood degraded by *P. sanguineus* after 12 weeks, despite weight loss similar to the other fungi, may thus be the result of the preferential degradation of non-crystalline hemicelluloses and lignin that characterize selective white rot (Zabel & Morrell 1992). However, this difference in pure cellulose content between *P. sanguineus* and *I. lacteus* after 12 weeks of decay was not detected in the carbohydrate analysis, presumably because this method does not differentiate between glucan resulting from crystalline *versus* non-crystalline materials (Fig 1).

The combination of non-enzymatic and enzymatic mechanisms in brown rot decay is expected to produce more effective and efficient degradation than solely enzymatic decay. However, at week 9 the brown rot *G. trabeum* and the white rot *I. lacteus* display similar percent crystallinities and similar weight losses (Martínez *et al.* 2011). One explanation for this may be that *G. trabeum* did in fact cause a more thorough hydrolysis of the wood material compared to *I. lacteus*, but this is balanced out by an increase in crystallinity caused by a preferential removal of the amorphous material by the brown rot fungus. The sum of these two effects would result in no significant change in the overall percent crystallinity caused by *G. trabeum* relative to *I. lacteus* and the undecayed control ($P = 0.7$ and $P = 0.9$, respectively). The lack of difference in crystallinity between the *G. trabeum* and *I. lacteus* even at week 12 ($P = 0.14$) may also be due to the fact that the greater depolymerization of the cellulose microfibrils does not necessarily cause a measurable reduction in crystallinity by XRD (Haw & Schultz 1985; Green *et al.* 1992; Hall *et al.* 2010). In addition, the presence of compounds such as cellulose binding modules (CBM), swollenin, and other expansin-like proteins have recently been found to add to the efficiency of the white rot fungi (Arantes & Saddler 2010). Also, the energy expended in producing enzymatic systems *versus* non-enzymatic systems by fungi has not been determined; however, enzymatic systems are known to be energetically expensive to organisms and are limited by low nitrogen environments such as those typically found in wood. More energetically efficient degradation may occur in some types of brown rots that rely more on non-enzymatic systems (Eastwood *et al.* 2011).

In order to confirm the changes in crystallinity determined using XRD, changes in the NMR spectral regions assigned to the C4 and C6 carbons in cellulose were examined. The PCA score plots and loadings are displayed in Fig 5. PC1 describes 93.4 % of the spectral variation, while 2.83 % of the variation is described by the second PC (PC2). The loading for PC1 is primarily due to C4 and C6 in cellulose, although resonances

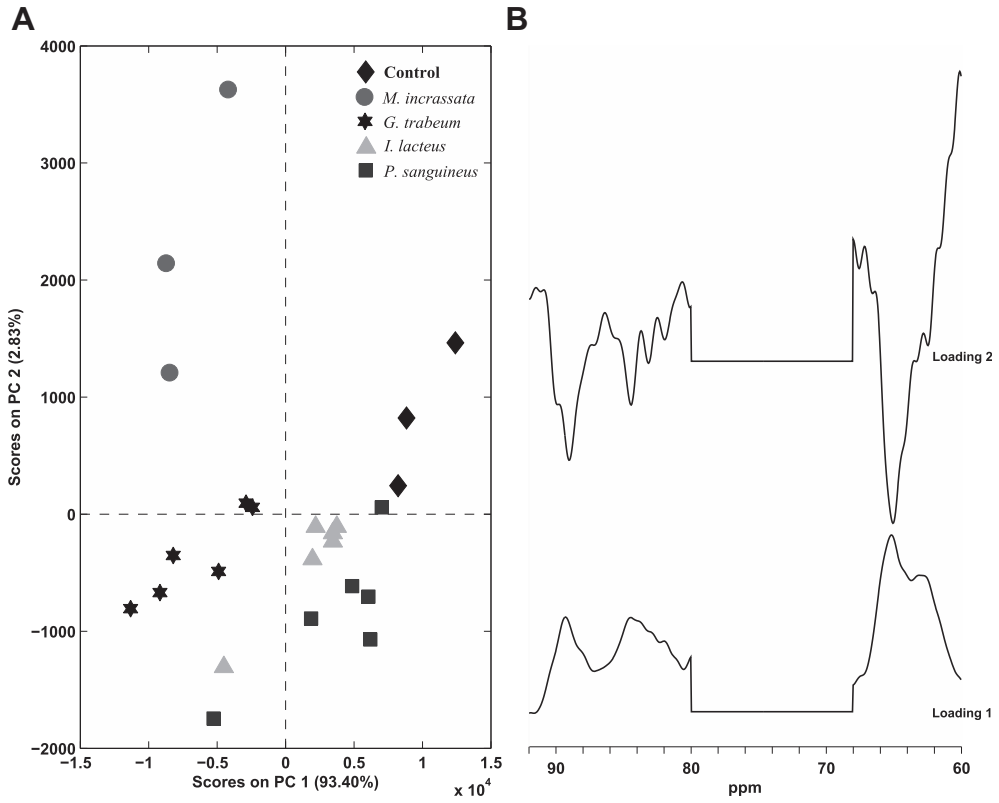

Fig 5 – Changes in C4 and C6 carbons. PCA of the ^{13}C CP/MAS spectra for the two areas originating from cellulose C4 (80–92 ppm) and cellulose C6 (60–68 ppm) using samples from week 9 (all fungi) and week 12 (only *G. trabeum*, *I. lacteus*, *P. sanguineus*, controls). Part (A) displays the score plot, and part (B) the corresponding loadings for the selected PCs.

from lignin and hemicelluloses are also contributing. The loading for PC2 represents the difference spectrum between lignin (and non-crystalline cellulose) and crystalline cellulose. Compared to the control samples a more negative PC2 score indicates a higher content of crystalline cellulose. The more positive PC2 score for the wood degraded by *M. incrassata* indicates less crystalline material in these samples than the others, in agreement with the percent crystallinity results (Fig 4). A lower score on PC1 compared to the control samples translates into lower cellulose content. The reduction in cellulose appears to be generally greater for the brown rot degraded wood and less for the white rot, despite similar weight losses. The degradation of the three major wood components by the white rot fungi is seen to result in a higher ratio of remaining cellulose to lignin materials, compared to the wood exposed to brown rot decay, preferentially removing hemicelluloses and cellulose (Fig 2). This corresponds to the findings from the carbohydrate and lignin analysis (Fig 1).

Changes in d-spacing

The brown rot fungi caused a significant rightward shift of the 22° 2θ peak assigned to the 200-plane of crystalline cellulose after 6 weeks of decay. This indicates a reduction in the average *d*-spacing between the crystalline planes ($P < 0.01$) (Fig 6). *Pycnoporus sanguineus* caused a significant increase in *d*-spacing initially in the decay process ($P = 0.007$) followed by a continuous decrease, although the final change in *d*-spacing value was less than what was observed for the brown rot fungi. For wood samples inoculated with *Irpex lacteus* a significant increase was seen at 12 weeks of decay ($P = 0.01$) (Fig 6).

The results suggest that the changes seen in *d*-spacing of the cellulose crystalline structure caused by these four species appear to be largely dependent on the type of decay mechanisms involved. The decrease in *d*-spacing is believed to be largely due to the removal of the loosely packed, frayed outer non- or para-crystalline material, resulting in the remaining crystalline regions that are highly ordered and tightly packed (Howell *et al.* 2009a, 2011). These regions have a higher surface area of exposure of crystalline materials and thus give a stronger XRD signal resulting in a higher 2-θ angle. This hypothesis is supported by the sugar analysis data shown in Fig 1, which show a similar decrease in the non-crystalline hemicellulose components of xylan and mannan for *Gloeophyllum trabeum* and *Meruliporia incrassata*. Further depolymerization of the cellulose chains of the crystals may allow the remaining crystalline material the freedom to relax into a more energetically favourable, tightly packed state (Howell *et al.* 2011) made possible by microfibril twisting (Matthews *et al.* 2011). The process of non-enzymatic decay likely aids these changes. The oxidizing power of the highly reactive hydroxyl radicals (•OH/−OH) originating from the modified Fenton reaction catalyzed by low molecular weight chelators depolymerizes polysaccharides *via* hydrogen abstraction as the hydroxyl groups are involved in a number of intra- and intermolecular hydrogen bonds, which determines the crystalline arrangements (Howell *et al.* 2007).

The increase in *d*-spacing observed in the white rot decayed samples at week 3 for *P. sanguineus* and week 12 for *I. lacteus* may be linked with the enzymatic processes of the white rot decay mechanism, which involves carbohydrate-binding modules (CBM) and cellobiohydrolase (Arantes & Saddler 2010). The CBM/cellobiose enzyme system is known to cause a 'swelling' of the tightly bound cellulose chains and to act processively, thus opening the structure and possibly causing the increased distance between the planes observed for the white rot fungi in Fig 6 (Arantes & Saddler 2010; Matthews *et al.* 2011). Only a few of these types of systems have been reported from brown rot fungi (Martinez *et al.* 2009). The relatively small magnitude of the change in *d*-spacing compared to the distance between the crystalline planes is likely due to the fact that the method of measurement (XRD) is an averaging technique, taking into account the crystal plane spacing throughout the entire sample. As the mechanisms suggested here would decrease the *d*-spacing only in the outermost cellulose chains, and even then not in every cellulose crystal, the actual change observed would be expected to be quite small.

Changes in interior/exterior cellulose ratio of C4

The change in ratio between interior and surface microfibril cellulose was analyzed *via* NMR by integration of the spectral regions at 86–92 and 80–86 ppm assigned to C4. Changes in the integrated areas of these regions describe the action of

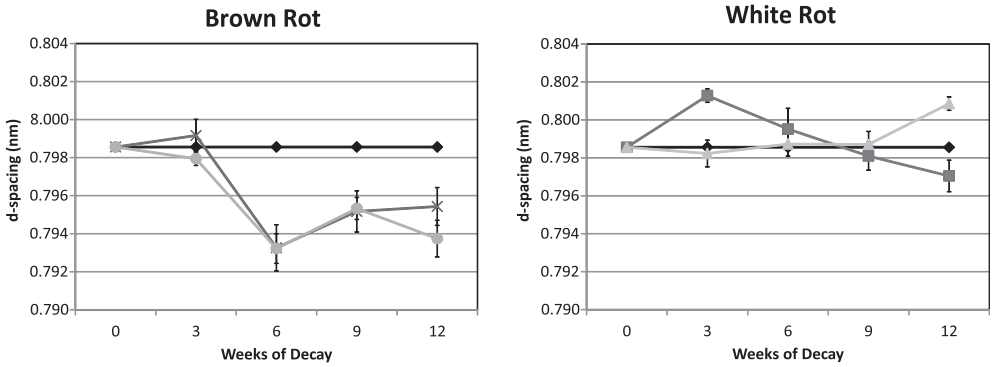

Fig 6 – Changes in *d*-spacing. Average (200-plane) *d*-spacing values as determined by XRD data for wood decayed by the brown rot fungi *M. incrassata* (circle) and *G. trabeum* (star) (left), and the white rot fungi *I. lacteus* (triangle) and *P. sanguineus* (square) (right) *versus* undecayed controls (diamond). Data for *M. incrassata* has been previously published (Howell *et al.* 2011).

Table 3 – Reduction in integrated area of the peaks at 86–92 ppm and 80–86 ppm corresponding to interior and surface cellulose, respectively, relative to control samples.

Weight loss	~20 %		~30 %	
Cellulose	Interior	Surface	Interior	Surface
G. trabeum	0.79 ± 0.03	0.75 ± 0.02	0.66 ± 0.05	0.66 ± 0.04
M. incrassata	[a]	[a]	0.66 ± 0.05	0.71 ± 0.07
I. lacteus	0.86 ± 0.01	0.89 ± 0.01	0.76 ± 0.10	0.83 ± 0.09
P. sanguineus	0.90 ± 0.04	0.93 ± 0.01	0.79 ± 0.12	0.84 ± 0.10
Control	1.00	1.00	1.00	1.00

a Blocks inoculated with *M. incrassata* did not display 20 % weight loss at any of the time points tested.

the degradative systems of the fungal species in terms of the direct action on the non-crystalline surface *versus* crystalline interior of the cellulose microfibrils. The reduction in both interior and surface microfibrils at 20 and 30 % weight loss was found to be higher in wood degraded by the two brown rot fungi compared to wood degraded by the two white rot fungi (Table 3). This result is possibly due to initiation of depolymerization of more recalcitrant components caused by low molecular weight compounds employed by brown rot fungi during decay. These results support the XRD analysis indicating a greater reduction in cellulose crystallinity by the brown rot fungi at later stages of decay. The difference seen for the two white rot fungi at ~20 % weight loss may be due to variation in weight loss (*Irpex lacteus* = 21.4 %, *Pycnoporus sanguineus* = 16.7 %) or the actual decay mechanism, e.g. simultaneous *versus* selective white rot.

There was no statistical difference in the reduction of interior crystalline cellulose (86–92 ppm) *versus* surface materials (80–86 ppm) of wood exposed to the two brown rot fungi at ~30 % weight loss ($P > 0.3$) (Table 3). At ~20 % weight loss *Gloeophyllum trabeum* cause a greater reduction in the surface (0.75) compared to interior region (0.79), and this is in agreement with the previous increase in the percent crystallinity calculated from XRD results (Howell *et al.* 2007, 2009a). These results are consistent with the data from the XRD analysis showing a decrease in the average *d*-spacing, as the relative increase in interior to surface ratio found for *G. trabeum* at 20 % weight loss would result in the reported peak shift at 22° 2θ and lower the average *d*-spacing. Due to the aggressiveness of the *Meruliporia incrassata* strain used, it was not possible to examine the ratios over time for this brown rot fungus. The same observation of a relative increase in core material was not seen in the white rot fungi, which displayed a constant relatively higher reduction of the components in the interior region.

Conclusion

Analysis of wood undergoing decay by the brown rot fungi *Gloeophyllum trabeum* and *Meruliporia incrassata*, and the white fungi *Irpex lacteus* and *Pycnoporus sanguineus* showed distinct variations both within and between the two types of fungi when analyzed for wood carbohydrate and lignin, using XRD and ^{13}C CP/MAS NMR analysis. The two brown rot fungi and the white rot fungus *I. lacteus* were found to decrease the percent crystallinity and the extent to which both the crystalline and non-crystalline wood components were removed dependent on the stage of decay. In contrast, the white rot fungus *P. sanguineus* was found to slightly increase the percent crystallinity at weeks 6 and 9, likely due to the selective removal of non-crystalline lignin and hemicelluloses caused by this species. These results correlate with the general understanding of the decay mechanisms proposed for these fungi.

The change in distance between the 200-crystal plane (*d*-spacing) of the cellulose crystals during decay was also found to differ, with the two brown rot fungi significantly decreasing the *d*-spacing relatively early in the decay process. In contrast, the two white rot fungi displayed a less consistent pattern generally displaying an increased crystalline spacing at different stages of the decay. These changes may be caused in part by the ability of the brown rot fungi to generate non-enzymatic decay mechanisms, which can penetrate the structure of the cellulose microfibrils *versus* the ability of the white rot fungi to produce specialized enzymes with less diffusion of low molecular weight systems. The white rot system initiates a surface attack on the cellulose but over time produces a swelling of the cellulose chain structure. Further studies employing more fungal species and isolates are needed in order to verify these results.

The results from this study emphasize the distinct substrate modifications caused by different fungal species and fungal types during the decay process. These changes can help in uncovering the mechanisms involved in the development of biological pretreatment methods for biomass in the production of ecologically sustainable fuels and biochemicals.

Acknowledgements

We thank David Frankel, UMaine for assistance with the X-ray diffraction instrumentation; Merian Haugwitz for assisting with statistical analysis. Martin F. Stoner for providing the original *Meruliporia incrassata* strain. Anne Christine Steenkjær Hastrup acknowledges support from the University of Copenhagen PhD Scholarship. Caitlin Howell acknowledges support from a US NSF Graduate Research Fellowship.

REFERENCES

American Wood Preservers' Association, 2003. Standard method of testing wood preservatives by laboratory soil-block cultures. In: *Book of Standards*. American Wood Preservers' Association, Granbury, TX, pp. 206–212.

Arantes V, Milagres AMF, Filley TR, Goodell B, 2011. Lignocellulosic polysaccharides and lignin degradation by wood decay fungi: the relevance of nonenzymatic Fenton-based reactions. *Journal of Industrial Microbiology and Biotechnology* **38**: 541–555.

Arantes V, Qian Y, Milagres AMF, Jellison J, Goodell B, 2009. Effect of pH and oxalic acid on the reduction of Fe_3 by a biomimetic chelator and on Fe_3 desorption/adsorption onto wood: implications for brown-rot decay. *International Biodeterioration and Biodegradation* **63**: 478–483.

Arantes V, Saddler JN, 2010. Access to cellulose limits the efficiency of enzymatic hydrolysis: the role of amorphogenesis. *Biotechnology for Biofuels* **3**: 4.

Atalla R, VanderHart D, 1999. The role of solid state ^{13}C NMR spectroscopy in studies of the nature of native celluloses. *Solid State Nuclear Magnetic Resonance* **15**: 1–19.

Baldrian P, Valkov V, 2008. Degradation of cellulose by basidiomycetous fungi. *FEMS Microbiology Reviews* **32**: 501–521.

Baldrian P, 2008. Mini review: wood-inhabiting ligninolytic basidiomycetes in soils: ecology and constraints for applicability in bioremediation. *Fungal Ecology* **1**: 4–12.

Bardet M, Gerbaud G, Giffard M, Doan C, Hediger S, Pape LL, 2009. ^{13}C high-resolution solid-state NMR for structural elucidation of archaeological woods. *Progress in Nuclear Magnetic Resonance Spectroscopy* **55**: 199–214.

Bennett AE, Rienstra CM, Auger M, Lakshmi K, Griffin RG, 1995. Heteronuclear decoupling in rotating solids. *The Journal of Chemical Physics* **103**: 6951.

Cave ID, 1997. Theory of X-ray measurement of microfibril angle in wood: part 2. *Wood Science and Technology* **31**: 225–234.

Cowling EB, 1961. *Comparative Biochemistry of the Decay of Sweetgum Sapwood by White-rot and Brown-rot Fungi*. US Department of Agriculture.

Cullity BD, 1978. *Elements of X-ray Diffraction*. Addison–Wesley Publishing Co., Inc, Reading, MA.

Curling S, Clausen C, Winandy J, 2001. The effect of hemicellulose degradation on the mechanical properties of wood during brown rot decay. *International Research Group on Wood Preservation* IRG/WP 01-20219.

Dutton MV, Evans CS, 1996. Oxalate production by fungi: its role in pathogenicity and ecology in the soil environment. *Canadian Journal of Microbiology* **42**: 881–895.

Eastwood DC, Floudas D, Binder M, Majcherczyk A, Schneider P, Aerts A, Asiegbu FO, Baker SE, Barry K, Bendiksby M, Blumentritt M, Coutinho PM, Cullen D, de Vries RP, Gathman A, Goodell B, Henrissat B, Ihrmark K, Kauserud H, Kohler A, LaButti K, Lapidus A, Lavin JL, Lee Y-H, Lindquist E, Lilly W, Lucas S, Morin E, Murat C, Oguiza JA, Park J, Pisabarro AG, Riley R, Rosling A, Salamov A, Schmidt O, Schmutz J, Skrede I, Stenlid J, Wiebenga A, Xie X, Kües U, Hibbett DS, Hoffmeister D, Högberg N, Martin F, Grigoriev IV, Watkinson SC, 2011. The plant cell wall decomposing machinery underlies the functional diversity of forest fungi. *Science* **333**: 762–765.

Flournoy DS, Kirk TK, Highley T, 1991. Wood decay by brown-rot fungi: changes in pore structure and cell wall volume. *Holzforschung* **45**: 383–388.

Goodell B, Jellison J, Liu J, Daniel G, Paszczynski A, Fekete F, Krishnamurthy S, Jun L, Xu G, 1997. Low molecular weight chelators and phenolic compounds isolated from wood decay fungi and their role in the fungal biodegradation of wood. *Journal of Biotechnology* **53**: 133–162.

Goodell B, Qian Y, Jellison J, Richard M, Qi W, 2002. Lignocellulose oxidation by low molecular weight metal-binding compounds isolated from wood degrading fungi: a comparison of brown rot and white rot systems and the potential application of chelator-mediated Fenton reactions. *Progress in Biotechnology* **21**: 37–47.

Green III F, Clausen CA, 2003. Copper tolerance of brown-rot fungi: time course of oxalic acid production. *International Biodeterioration and Biodegradation* **51**: 145–149.

Green III F, Larsen M, Hackney J, Clausen C, Highley T, 1992. Acid-mediated depolymerization of cellulose during incipient brown-rot decay by *Postia placenta*. In: Kuwahara M, Shimada M (eds), *Biotechnology in the Pulp and Paper Industry*. Uni Publishers, Kyoto, Japan.

Hall M, Bansal P, Lee JH, Realff MJ, Bommarius AS, 2010. Cellulose crystallinity – a key predictor of the enzymatic hydrolysis rate. *FEBS Journal* **277**: 1571–1582.

Hammel KE, Kapich AN, Jensen KA, Ryan ZC, 2002. Reactive oxygen species as agents of wood decay by fungi. *Enzyme and Microbial Technology* **30**: 445–453.

Hastrup ACS, 2011. *Aspects of Cellulose Degradation by Brown Rot Fungi – involvement of enzymatic and non-enzymatic decay processes including oxalic acid regulation and metal sequestering*. Dissertation, University of Copenhagen, Denmark.

Hastrup ACS, Green III F, Clausen CA, Jensen B, 2005. Tolerance of *Serpula lacrymans* to copper-based wood preservatives. *International Biodeterioration and Biodegradation* **56**: 173–177.

Hastrup ACS, Howell C, Jensen B, Green III F, 2011. Non-enzymatic depolymerization of cotton cellulose by fungal mimicking metabolites. *International Biodeterioration and Biodegradation* **65**: 553–559.

Hastrup ACS, Jensen B, Clausen C, Green III F, 2006. The effect of $CaCl_2$ on growth rate, wood decay and oxalic acid accumulation in *Serpula lacrymans* and related brown-rot fungi. *Holzforschung* **60**: 339–345.

Hastrup ACS, Jensen TØ, Jensen B, 2012a. Detection of iron-chelating and iron-reducing compounds in four brown-rot fungi. *Holzforschung*, in press.

Hastrup ACS, Green F III, Lebow P, Jensen B, 2012b. Enzymatic oxalic acid regulation correlated with wood degradation in four brown rot fungi. *International Biodeterioration and Biodegradation*, in press.

Haw JF, Schultz TP, 1985. Carbon-$^{13}CP/MAS$ NMR and FT-IR study of low-temperature lignin pyrolysis. *Holzforschung* **39**: 289–296.

Highley T, 1976. Hemicellulases of white- and brown-rot fungi: time course of oxalic acid production. *Material und Organismen* **11**: 33–46.

Himmel ME, Ding SY, Johnson DK, Adney WS, Nimlos MR, Brady JW, Foust TD, 2007. Biomass recalcitrance: engineering plants and enzymes for biofuels production. *Science* **315**: 804–807.

Howell C, Hastrup ACS, Goodell B, Jellison J, 2009a. Temporal changes in wood crystalline cellulose during degradation by brown rot fungi. *International Biodeterioration and Biodegradation* **63**: 414–419.

Howell C, Hastrup ACS, Jara R, Larsen FH, Goodell B, Jellison J, 2011. Effects of hot water extraction and fungal decay on wood crystalline cellulose structure. *Cellulose* **18**: 1179–1190.

Howell C, Hastrup ACS, Jellison J, 2007. The use of X-ray diffraction for analyzing biomodification of crystalline cellulose by wood decay fungi. *International Research Group on Wood Preservation* IRG/WP 07–10622.

Howell C, Paredes JJ, Jellison J, 2009b. Decay resistance properties of hot water extracted oriented strandboard. *Wood and Fiber Science* **41**: 201–208.

Hyde SM, Wood PM, 1997. A mechanism for production of hydroxyl radicals by the brown-rot fungus *Coniophora puteana*: Fe (III) reduction by cellobiose dehydrogenase and Fe (II) oxidation at a distance from the hyphae. *Microbiology* **143**: 259–266.

Kleman-Leyer K, Agosin E, Conner AH, Kirk TK, 1992. Changes in molecular size distribution of cellulose during attack by white rot and brown rot fungi. *Applied and Environmental Microbiology* **58**: 1266–1270.

Larsson PT, Wickholm K, Iversen T, 1997. A CP/MAS ^{13}C NMR investigation of molecular ordering in celluloses. *Carbohydrate Research* **302**: 19–25.

Lichtenegger H, Muller M, Paris O, Riekel CH, Fratzl P, 1999. Imaging of the helical arrangement of cellulose fibrils in wood by synchrotron X-ray micro-diffraction. *Journal of Applied Crystallography* **32**: 1127–1133.

Martínez AT, Rencoret J, Nieto L, Jiménez-Barbero J, Gutiérez A, del Río JC, 2011. Selective lignin and polysaccharide removal in natural fungal decay of wood as evidenced by in situ structural analyses. *Environmental Microbiology* **13**: 96–107.

Martínez ÁT, Speranza M, Ruiz-Dueñas FJ, Ferreira P, Camarero S, Guillén F, Martínez MJ, Gutiérrez A, Río JC, 2005.

Biodegradation of lignocellulosics: microbial, chemical, and enzymatic aspects of the fungal attack of lignin. *International Microbiology* **8**: 195–204.

Martinez D, Challacombe J, Morgenstern I, Hibbett D, Schmoll M, Kubicek CP, Ferreira P, Ruiz-Duenas FJ, Martinez AT, Kersten P, 2009. Genome, transcriptome, and secretome analysis of wood decay fungus *Postia placenta* supports unique mechanisms of lignocellulose conversion. *Proceedings of the National Academy of Sciences* **106**: 1954.

Matthews JF, Bergenstråhle M, Beckham GT, Himmel ME, Nimlos MR, Brady JW, Crowley MF, 2011. High-temperature behavior of cellulose I. *Journal of Physical Chemistry B* **115**: 2155–2166.

Moxley G, Zhang YHP, 2007. More accurate determination of acid-labile carbohydrates in lignocellulose by modified quantitative saccharification. *Energy and Fuels* **21**: 3684–3688.

Newman RH, Hemmingson JA, 1995. Carbon-13 NMR distinction between categories of molecular order and disorder in cellulose. *Cellulose* **2**: 95–110.

Nishiyama Y, 2009. Structure and properties of the cellulose microfibril. *Journal of Wood Science* **55**: 241–249.

Nishiyama Y, Langan P, Chanzy H, 2002. Crystal structure and hydrogen-bonding system in cellulose Iβ from synchrotron X-ray and neutron fiber diffraction. *Journal of the American Chemical Society* **124**: 9074–9082.

Pandey KK, Pitman AJ, 2003. FTIR studies of the changes in wood chemistry following decay by brown-rot and white-rot fungi. *International Biodeterioration and Biodegradation* **52**: 151–160.

Peersen OB, Wu X, Kustanovich I, Smith SO, 1993. Variable-amplitude cross-polarization MAS NMR. *Journal of Magnetic Resonance A* **104**: 334–339.

Rietveld HM, 1969. A profile refinement method for nuclear and magnetic structures. *Journal of Applied Crystallography* **2**: 65–71.

Schilling JS, Jellison J, 2006. Metal accumulation without enhanced oxalate secretion in wood degraded by brown rot fungi. *Applied and Environmental Microbiology* **72**: 5662–5665.

Sluiter A, Hames B, Ruiz R, Scarlata C, Sluiter J, Templeton D, Crocker D, 2008. Determination of structural carbohydrates and lignin in biomass. *Laboratory Analytical Procedure*, NREL/TP-510-42618.

Thygesen A, Oddershede J, Lilholt H, Thomsen AB, Ståhl K, 2005. On the determination of crystallinity and cellulose content in plant fibres. *Cellulose* **12**: 563–576.

Thygesen LG, Hidayat BJ, Johansen KS, Felby C, 2011. Role of supramolecular cellulose structures in enzymatic hydrolysis of plant cell walls. *Journal of Industrial Microbiology and Biotechnology* **38**: 975–983.

Tuor U, Winterhalter K, Fiechter A, 1995. Enzymes of white-rot fungi involved in lignin degradation and ecological determinants for wood decay. *Journal of Biotechnology* **41**: 1–17.

VanderHart DL, Atalla R, 1984. Studies of microstructure in native celluloses using solid-state carbon-13 NMR. *Macromolecules* **17**: 1465–1472.

Wold S, Esbensen K, Geladi P, 1987. Principal component analysis. *Chemometrics and Intelligent Laboratory Systems* **2**: 37–52.

Yelle DJ, Ralph J, Lu F, Hammel KE, 2008. Evidence for cleavage of lignin by a brown rot basidiomycete. *Environmental Microbiology* **10**: 1844–1849.

Yelle DJ, Wei D, Ralph J, Hammel KE, 2011. Multidimensional NMR analysis reveals truncated lignin structures in wood decayed by the brown rot basidiomycete *Postia placenta*. *Environmental Microbiology* **13**: 1091–1100.

Zabel RA, Morrell JJ, 1992. *Wood Microbiology: decay and its prevention*. Academic press, Inc., San Diego.

Zhao H, Kwak JH, Conrad Zhang Z, Brown HM, Arey BW, Holladay JE, 2007. Studying cellulose fiber structure by SEM, XRD, NMR and acid hydrolysis. *Carbohydrate Polymers* **68**: 235–241.